Irreversible transitions in a model substrate cycle

An experimental illustration

Alain Cimino and Jean-François Hervagault

Unité de Recherche Associée no. 523 du Centre National de la Recherche Scientifique, Université de Compiègne, Boite Postale no. 649, 60206 Compiègne, France

In a previous article [(1987) J. Theor. Biol, 127, 439–449], the dynamic behavior of a simple substrate cycle, bounded by moiety conservation, and in which one of the two antagonist enzymes is subjected to a destabilizing factor, was investigated. Depending upon the control parameter chosen, that is, the total interconverted substrate concentration and the ratio of the interconverting enzyme maximal activities, monostability, reversible (hysteresis) and/or irreversible transitions could be observed. In the present work, we report experiments dealing with the moiety ATP/ADP interconverted by enzymes phosphofructokinase (PFK) and pyruvate kinase (PK). The cycle operates under conditions where (1) PFK is inhibited by excess of its substrate, ATP, and (2) both enzymes are working under zero-order kinetics for their respective cosubstrates F6P and PEP. Under conditions where the PK maximal activity is lower than the PFK optimal activity, irreversible transitions from a high ATP (resp. low ADP) steady-state concentration to a lower (resp. higher) one, are observed when varying the total moiety (ATP + ADP) concentration. A graphical interpretation of the observed behavior is given. Plausible biochemical consequences of this phenomenon are also emphasized.

Bistability; Metabolic regulation

1. INTRODUCTION

Cyclic processes are ubiquitous in metabolism. They take place in many instances such as oxidation and synthesis, the generation of energy and reducing equivalents. These cycles occur when there are two opposing metabolic pathways in which the reaction(s) in the forward and reverse directions are catalyzed by different enzymes. If the simultaneous operation of these two interconverting enzymes leads to the hydrolysis of an energy-rich compound (e.g. ATP) with no net flux of metabolites, such cycles are designated as futile.

There is no doubt that substrate cycles actually occur within the cell [1]: these include glucose/glucose-6-phosphate, fructose-6-phosphate/fructose-1,6-bisphosphate, pyruvate/phosphoenol pyruvate [2–4], adenosine/AMP [5], glycogen/glucose-1-phosphate [6–8], glutamate/glutamine [9,10], triglycerides/fatty acids [11,12], along with the Ca^{2+} and Na^+ translocation cycles [12,13]. Furthermore, the process of protein synthesis and degradation can be considered to be an amino acids/protein cycle.

Another important feature of the (intermediary) metabolism is the existence of moiety-conserved cycles [14,15]. The two best known groups of metabolites participating in such operations are ATP/ADP and NAD(P)/NAD(P)H.

The role played by cycles (futile or not) in the regulation of metabolism is still a matter of controversy. However, from experimental data and theoretical considerations it is likely that substrate cycling is involved in thermogenesis [12,16], in the orientation of fluxes, in the control of concentrations [17], and in the amplification of sensitivity [18–21].

When dealing with cycles subject to a destabilising factor (product activation, substrate inhibition, etc.), more sophisticated dynamics may be observed, such as multistationarity (alternative steady-states), sustained oscillations or chaotic motions [15,22].

In connection with this latter aspect, we have studied theoretically the behavior of a model substrate cycle bounded by moiety-conservation [23]. When one of the interconverting enzymes is inhibited by an excess of its substrate, such a cycle can exhibit irreversible transitions. By irreversible transitions we mean that, contrarily to what occurs in a classical bistable system, the switching from one steady-state to the other is at most possible one time. These irreversibility features are in no way due to a bounded domain of variation of one parameter (experimental constraints and/or irrealistic physical meaning) but are an intrinsic property of the highly non-linear system considered.

Surprisingly, little attention has been paid to this interesting feature of dynamic systems as yet. In the frame of (bio)chemical systems, the rare reports related

Correspondence address: A. Cimino, Unité de Recherche Associée no. 523 du Centre National de la Recherche Scientifique, Université de Compiègne, Boite Postale no. 649, 60206 Compiègne, France

to this aspect basically deal with theoretical approaches or predictions. Studying analytically a Monod-Jacob model for induction and repression, Babloyantz and Nicolis [24] have shown that, if due to temporary metabolic advantages, a pathway is in a situation where it has a head start, all the other pathways will be inhibited permanently. Hahn et al. [25], when considering the dynamic behavior of a simple compartmentalized michaelian enzyme in which the product of the reaction alters the supply of substrate, mention some conditions under which irreversible transitions may occur. Later on, the same authors again take up this concept in order to attempt a plausible interpretation for the growth of crown gall tumors (personal communication).

Our aim in the present work is to show *experimentally* that in a simple model substrate cycle such irreversible transitions can be observed in the absence of any drastic constraints imposed on the enzyme kinetic properties and/or the parameter values.

1.2. *Model vs experimental*

Our goal is to illustrate experimentally certain particular dynamics behaviors of a previously described model cycle; we will first recall briefly its main features and conditions of validity. Two metabolites, S_1 and S_2, bounded by moiety-conservation ($S_1 + S_2 = S_T$) are converted in a cyclic manner by two enzymes, E_1 and E_2. Enzyme E_1 is inhibited by an excess of its substrate S_1. Because both enzymes require different cosubstrates, A and C, the two pathways are thermodynamically favorable at the same time. The enzyme kinetics are supposed to be zero-order with respect to their cosubstrates. In that cycle, the two control parameters are (1) the moiety total concentration, S_T, and (2) the ratio, V, of the interconverting enzymes' maximal activities. Monostability and reversible bistability (hysteresis) can be observed when either S_T or V are varied. Irreversible transitions occur when and only when S_T is taken as the control parameter. The only kinetic requirement is that the *maximal* activity of

the non-inhibited enzyme (E_2) is lower than the *optimal* activity of the inhibited one (E_1).

The model experimental system we have chosen is the interconversion of the moiety ATP/ADP (S_1/S_2) by enzymes phosphofructokinase (PFK = E_1) and pyruvate kinase (PK = E_2). Enzyme PFK exhibits an important inhibition by excess of its substrate, ATP. The standard Gibbs free energies ($\Delta G^{\circ\prime}$) of the reactions catalyzed by PFK (ATP + F-6-P $\longrightarrow$ ADP + F-1,6-diP) and PK (ADP + PEP $\longrightarrow$ ATP + Pyr) are -3.4 and -7.5 kcal·mol^{-1}, respectively. In order to ensure that cosubstrates, F6P (A) and PEP (C) are present at a constant level during the time course of the reactions prior to reach the steady-states, their initial concentrations are large with respect to their K_ms. The minimum model cycle and the experimental system are depicted in Fig. 1.

2. MATERIALS AND METHODS

The initial activity dependence of pyruvate kinase (PK; EC 2.7.1.40, from rabbit muscle) as a function of ADP was studied by using the pyruvate coupled assay. Measurements were performed in the presence of 5 mM phosphoenol pyruvate (PEP), 1 mM MgCl$_2$ and 0.3 mM NADH. The reaction was initiated by introduction of 1.5 and 3 IU·ml^{-1} PK and lactic dehydrogenase (LDH; EC 1.1.1.28), respectively.

For phosphofructokinase (PFK; EC 2.7.1.1, from rabbit muscle), the kinetic measurements were made by using the aldolase (ALD; EC 4.1.2.13)/triosephosphate isomerase (TPI; EC 5.3.1.1)/glycerol-3-phosphate dehydrogenase (NAD$^+$) (G-3-PdH; EC 1.1.1.8) coupled assay, in the presence of 1 mM MgCl$_2$, 1.1 mM F-6-P and 0.3 mM NAD$^+$. The amounts of the three coupling enzymes were 10–50-fold the maximal PFK activity, i.e. 0.07, 0.7, 3 and 3 IU·ml^{-1} for PFK, ALD, TPI and G-3-PdH, respectively. The increase in the NAD$^+$ concentration is followed at 340 nm.

The concentrations of F-6-P (PFK) and PEP (PK) were chosen such that the enzymes operate under zero-order conditions with respect to these substrates ([F-6-P] $\approx$ 16 K_m and [PEP] $\approx$ 45 K_m).

2.2. *Operation of the complete cycle*

The kinetic studies dealing with the complete bienzyme cycle, including PFK and PK, were carried out in a thermostated closed reactor (12 ml) containing F-6-P 1.1 mM, PEP 5 mM, and MgCl$_2$ 1 mM. Samples (0.5 ml) are taken at regular intervals, then diluted in a solution of acetonitrile/working buffer (1:2 v/v) up to a final volume of 2 ml, in order to stop the reactions. The samples can thus be stored congealed at $-20°C$. The steady-states are supposed to be attained when the difference in the ATP (ADP) concentrations between two consecutive samples is less than 5%.

2.3. *HPLC nucleosides determination*

The samples were centrifuged for 5 min at 2000 × g, and the supernatant was then filtered on a Millex filter (0.4 μm). A 100 μl aliquot of the filtrate was injected through an automatic sampler (WISP, Waters) into a SAX μBondapak Waters column, using a radical compressor module (8 × 10 Waters) under isocratic conditions. The elution solution is made of KH$_2$PO$_4$ 0.25 M and KCl 0.5 M at pH 4.0. Nucleoside mono-, di- and triphosphates were detected spectrophotometrically at 260 nm (LS Waters detector). Total elution was
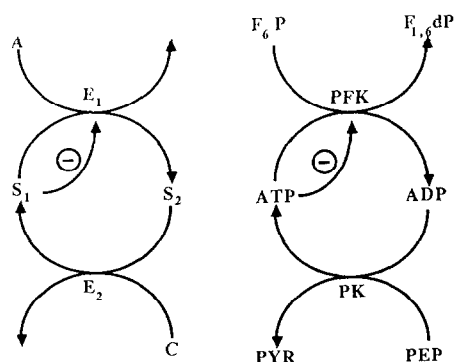

Fig. 1. The model minimal cycle and the experimental system under investigation.
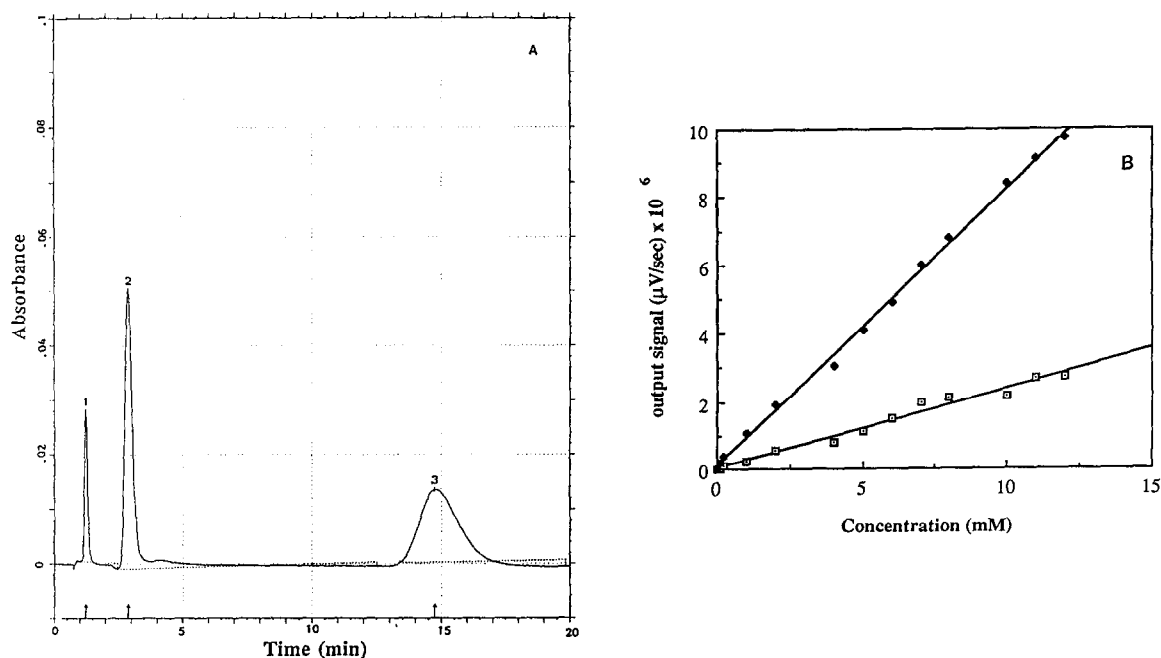
Fig. 2. (A) ATP (full symbols) and ADP (open symbols) calibration curves. The samples were treated as described in section 2. (B) Example of a chromatogram (Waters HPLC device output) showing the fairly good resolution of the various peaks. The sample contained 0.01, 0.1 and 0.2 mM AMP (1), ADP (2) and ATP (3), respectively.

achieved in 17 min. Each detection was carried out twice and each sample was doubled. The calibration curves for ATP and ADP along with an elution profile example are shown in Fig. 2A and B.

3. RESULTS AND DISCUSSION

The activity of the two converting enzymes, PFK and PK, as a function of ATP and ADP, respectively, in the presence of saturating concentrations of their respective cosubstrates (F-6-P and PEP), are shown in Fig. 3A and B. A detailed (mechanistic) description of the actual enzyme kinetics is not essential to explain the observations, insofar as our aim is just to illustrate experimentally the qualitative behavior of a model system. Thus, for the purpose of the present work and under our experimental conditions, the rate expressions of the two enzymes can be described by classical one-substrate Michaelis equations. For PKF, this equation is corrected by addition of a term accounting for the substrate (ATP) competitive inhibition.

$$v_{PFK} = V_{mPFK} \frac{[ATP]}{K_{mATP} + [ATP] + \dfrac{[ATP]^2}{K_{iATP}}}$$

and

$$v_{PK} = V_{mPK} \frac{[ADP]}{K_{mADP} + [ADP]} \qquad (1)$$

In these equations, the square brackets stand for the concentrations. By conservation arguments, [ADP] can

be replaced by ([AXP]$_T$ − [ATP]), where [AXP]$_T$ represents the total concentration of the moieties (ATP + ADP).

Non-linear regression analysis carried out on the experimental data points gave the following values for the kinetic constants: $K_{mATP} = 47$ μM, $K_{iATP} = 837$ μM and $K_{mADP} = 1.39$ mM with $r^2 > 0.98$.

In addition, the optimal PFK activity (v_{optPFK}) is calculated according to

$$v_{optPFK} = V_{mPFK} \frac{2K_{mATP}}{(K_{mATP}K_{iATP})^{1/2}} + 1 \qquad (2)$$

Since the concentration of (ATP + ADP) is constant, the representative functions of v_{PFK} and v_{PK} can be plotted on the same graph. The steady-state(s) of the cycle are defined by the intersections of the two curves. The actual maximal enzyme activities are chosen such that V_{mPK} is lower than V_{optPFK}. The representative curves of v_{PFK} and v_{PK} as a function of various concentrations of AXP$_T$ are shown in Fig. 4A.

For the sake of clarity, v_{PFK} as a function of [ATP](= [AXP]$_T$ − [ADP]) is referred to as curve A, and v_{PK} as a function of [ADP](= [AXP]$_T$ − [ATP]) are referred to as curves B, C and D (various [ATP]$_T$).

In this graphical representation, v_{PK} (ADP —→ATP) equals zero when [ATP] = [AXP]$_T$. Given an [AXP]$_T$ value, curve A and curves B, C or D can have one (B), two (C) or three (D) intersection points. The ordinate and abscissa of each of these points correspond to the steady-state velocities and ATP (ADP) concentrations,
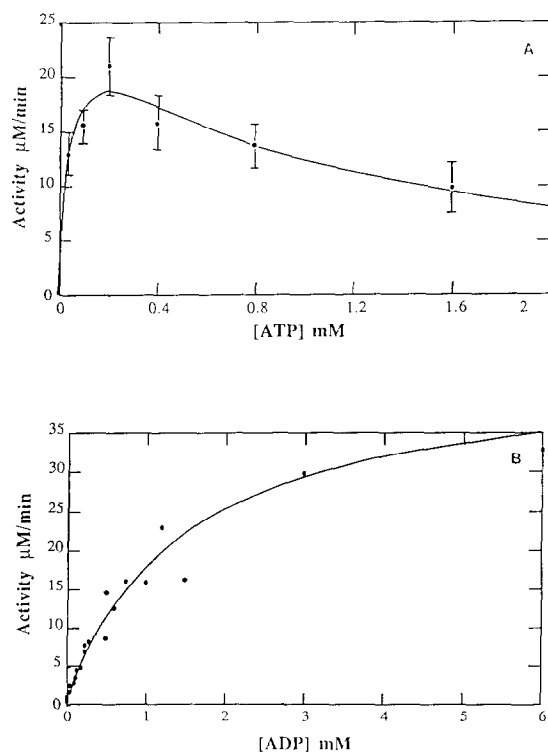
Fig. 3. Velocity curves of enzymes PFK as a function of [ATP] in the presence of 1.1 mM F-6-P (A) and PK as a function of [ADP] in the presence of 5 mM PEP (B). The lines through the experimental data points are the best fits calculated from Eqn 1 using a non-linear regression analysis.

respectively. Therefore, the cycle can have one (stable), two (stable) or three (two stable and one unstable) steady-state solutions.

When considering the situation where bistability occurs (e.g. curves C and D), one or the other of the two

stable steady-states observed will depend on the initial conditions imposed on the system. As an example, let us consider curves A and D in Fig. 4A. The system has 3 intersections (points labelled 3, 6 and 8), among which only the abscissa of points 3 and 8 correspond to stable ATP (ADP) steady-state concentrations. If, at time zero, [AXP]$_T$ is only composed of ADP ([ATP] = 0), then point 3 will be attained. Conversely, if the initial [AXP]$_T$ is only composed of ATP ([ADP] = 0), the steady-state will correspond to point 8.

Let us now look at the path followed by an intersection point (steady-state) when [AXP]$_T$ is varied. Starting from point 8, on the right-hand branch of curve A, and decreasing [AXP]$_T$, this point will move on that branch down to point 7. A further decrease in [AXP]$_T$ will cause a jump (discontinuity) of the point onto the left-hand branch of A. Its final location will be zero. If [AXP]$_T$ is now increased from zero up to higher concentrations, the point will follow the path 1, 2, 3 and 4 (asymptotic value for infinite [AXP]$_T$). The important point here is that due to the restrictive condition, $v_{optPFK} > V_{mPK}$, the system is in no way able to return to a situation corresponding to points 7 and 8. In other words, no loop can be described by varying cyclically a parameter ([AXP]$_T$), as it would be the case with a classical reversible bistable (hysteresis). Irreversibility occurs after the transition $7 \longrightarrow 1$.

The successive situations just described can be summarized by plotting the ATP (ADP) steady-state concentrations (abscissa of the intersection points) as a function of [AXP]$_T$ (Fig. 4B). The full and dashed lines correspond to stable and unstable steady-state solutions, respectively. The lower stable and the intermediary unstable branches tend to asymptotic values of [ATP] (abscissa of points 4 and 5, respectively),
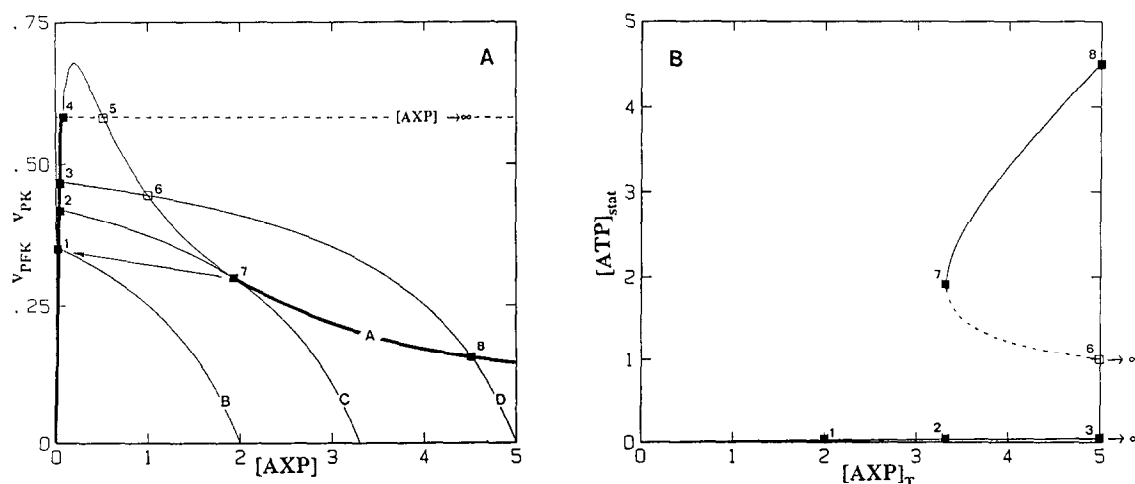

Fig. 4. (A) Graphical determination of the steady-states of the cycle. v_{PFK} (curve A) and v_{PK} (curves B, C and D) are plotted as a function of [AXP]. The dashed curve (part) represents v_{PK} at infinite ADP concentrations. Full and open squares correspond to the stable and unstable steady-states. The heavy lines indicate the loci of stable steady-states actually observed (stable) when ATP (ADP) is varied increasingly and/or decreasingly. The jump from point 7 to point 1 (arrow) is irreversible. (B) Steady-state ATP concentrations as a function of [AXP]$_T$. Points 5 and 6 are located on the intermediary (unstable) branch. Point 7 is identified as the only existing limit (turning) point.

whose analytical expressions are straightforward. From this figure, the ability of a unique and irreversible transition appears clearly.

A way to confirm experimentally this behavior consists of determining the ATP (ADP) steady-state concentrations for various $[AXP]_T$. In order to check (and determine) the existence of one or two stable states at a given $[AXP]_T$, each evolution has to be made with two different initial conditions, that is, e.g. $[ATP]_{init} = 0$ (the whole pool of adenosine phosphates is in the form of ADP), and $[ATP]_{init} = [AXP]_T$. Fig. 5a–f shows the evolution of the ATP and ADP concentrations for $[AXP]_T$ equal to 3, 6 and 12.6 mM. In these

experiments, the PFK and PK maximal activities equal $78\,\mu\mathrm{M}\cdot\mathrm{min}^{-1}$ ($v_{optPFK} = 53\,\mu\mathrm{M}\cdot\mathrm{min}^{-1}$) and $32\,\mu\mathrm{M}\cdot\mathrm{min}^{-1}$ ($< v_{optPFK}$), respectively. For $[AXP]_T$ equal to 3 mM, the same ATP (ADP) steady-state concentration is reached ($60\,\mu\mathrm{M}$ (2.94 mM)), regardless of the initial conditions ($[ATP]_{init} = 0$ or $[ADP]_{init} = 0$). For $[AXP]_T$ equal to 6 and 12.6 mM, the steady-state concentrations depend upon the initial ATP (ADP) conditions. Fig. 5c (see also Fig. 5d, for ADP) shows the ATP concentration evolution for $[AXP]_T = 6$ mM when starting with either $[ATP]_{init} = [AXP]_T$ (empty symbols) or $[ATP]_{init} = 0$ ($[ADP]_{init} = [AXP]_T$, full symbols). In the first case the steady-state concentra-
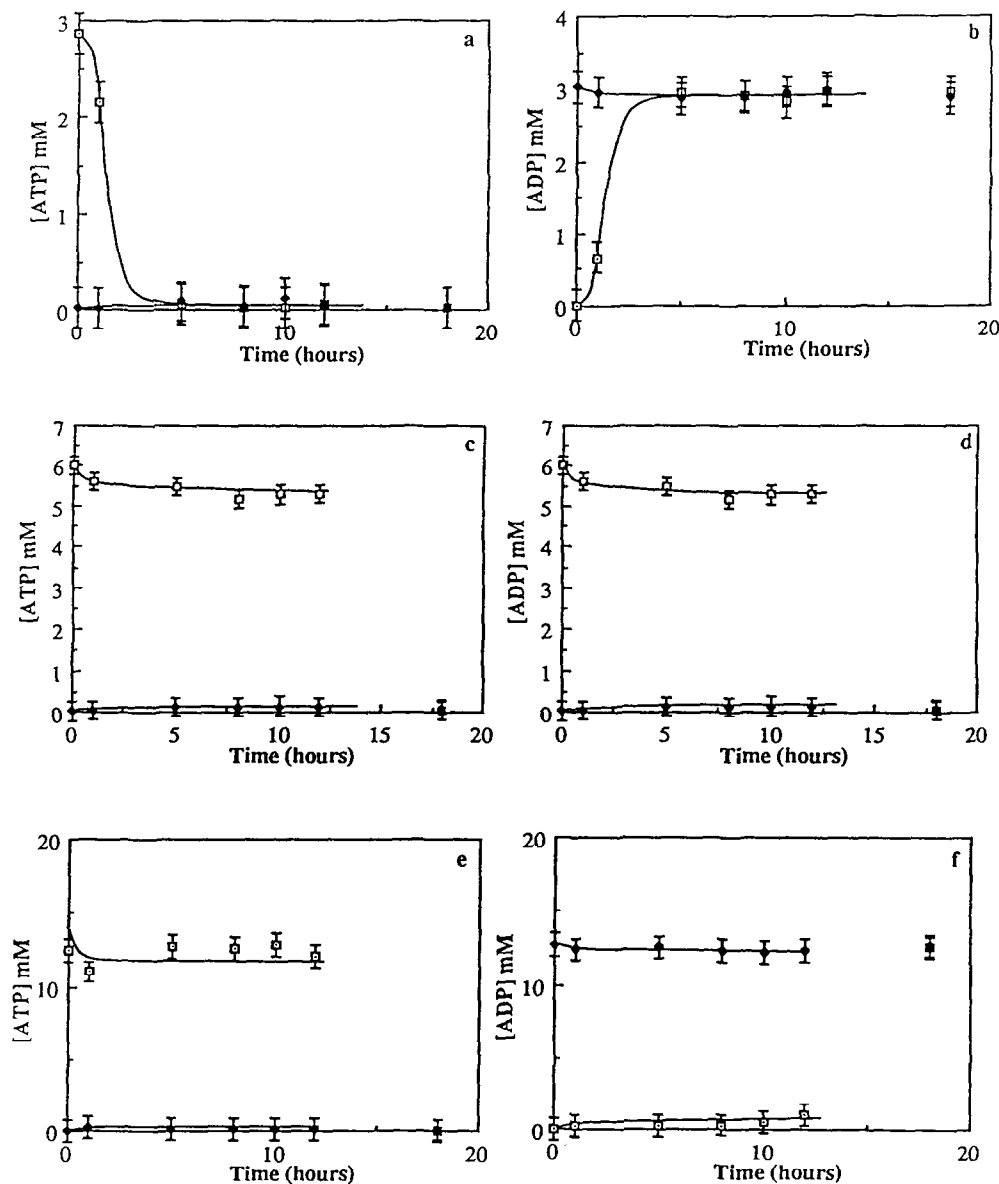

Fig. 5. Evolution of the ATP (a, c, e) and ADP (b, d, f) concentrations for the PFK/PK cycle. The nucleoside concentrations are determined by HPLC measurements. In each figure open and full symbols represent the evolution of concentrations for $[ATP]_{init} = [AXP]_T$ (absence of initial ADP) and $[ADP]_{init} = [AXP]_T$ (absence of initial ATP), respectively. (a) and (b) $[AXP]_T = 3$ mM. One single steady-state is observed, regardless of the initial conditions. (c) and (d) $[AXP]_T = 6$ mM. (e) and (f) $[AXP]_T = 12.6$ mM. Depending upon the initial nucleoside composition, two different stable steady-states can be reached. In any case, V_{mPK} and V_{mPFK} equal 32 and $78\,\mu\mathrm{M}\cdot\mathrm{min}^{-1}$, respectively.
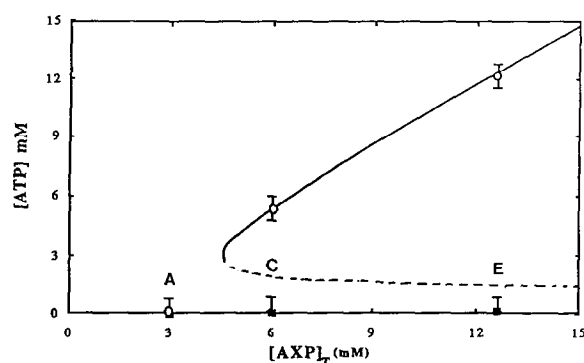
Fig. 6. Experimentally observed ATP steady-state concentrations (see Fig. 5) plotted as a function of $[AXP]_T$. The curve drawn through the data points was calculated from Eqn 1 with the actual parameter values and the enzyme maximal activities as in Fig. 5.

tion is reached for [ATP] = 5.3 mM, and in the second one it equals 0.13 mM. A qualitatively similar behavior is observed when $[AXP]_T$ equals 12.6 mM (Fig. 5e and f, [ATP] = 11.9/0.35 mM).

The experimentally measured ATP steady-state concentrations as a function of $[AXP]_T$ are reported in Fig. 6. The curve drawn through the data points was calculated from the actual experimental parameter values. It is noteworthy that the model predictions agree fairly well with the observations. However, this very agreement is, to some extent, a little frustrating insofar as it cannot bring a definitive demonstration of the phenomenon: indeed, the model predicts that two stable steady-states coexist when $[AXP]_T$ tends to infinity. Experiments carried out in the presence of very high ATP (ADP) concentrations are obviously inachievable.

4. CONCLUSION

Preliminary calculations dealing with the same system, but open to mass transfers (compartmentalization and/or flow-through reactors) show that a qualitatively similar behavior (occurrence of irreversible transitions) can occur not only when $[AXP]_T$ is varied, but also when the ratio of the two converting enzyme maximal activities is taken as the control parameter (in preparation).

The model bienzyme system described in this work is the first attempt at showing experimentally that a binary model cycle interconverting two substrates by two antagonist enzymes may exhibit irreversible transitions. Obviously, examples of such cycles are ubiquitous in metabolic pathways. But the meaning of 'substrate' must be taken in its broadest sense: one may deal with cofactors recycling (ATP, as here, GTP, NAD(P), AcCoA, etc.), with pathway intermediates, or even with protein covalent modifications (phosphorylation, methylation, etc.). The global dynamic features of such cycles may also account, in a

qualitative way, for more complex networks involving numerous catalytic steps in each direction, with or without compartmentalization. The non-linearities may arise from the resulting effect of several cross-feedbacks. Thus far, one may put forward some new interesting insights on the behavior of interacting pathways such as glycolysis/glyconeogenesis (futile cycling), glycolysis/respiratory chain (redox cycling) or shuttles (malate/aspartate). Such correlations between enzymic pathways have already been emphasized regarding the regulation of synthesis of proteins [26]. The compartmentalization, if involved, may not be limited to subcellular elements but extended to connecting cells and/or organs (e.g. Cori cycle).

By keeping in mind these various plausible situations, one may view some hypotheses regarding the relevance and the metabolic implications of irreversible transitions. Such transitions may be either advantageous for the cell, in that they can represent a simple and efficient emergency mechanism for adapting to profound changes in the environment, or disadvantageous, with pathological consequences. These transitions may also be involved in differentiation processes. Whatever the origins and/or the underlying mechanisms might be, they can induce the selection of one pathway at the expense of the other, which will remain permanently inhibited. Rashevsky [27] has described an oxygen starvation experiment on yeast cells which brings about a transformation of the cells from one metabolic state to another. It is also plausible that, in genetically identical cellular lines, epigenetic differences (post-transcriptional events) may result in a divergence from a common initial situation and persisting indefinitely in numerous states of regime. Some documented cases of these epigenetic differences have been found to occur in microorganisms [28–30]. Recently, Kaufman and Thomas [31] have shown that three stable steady-state concentrations of T lymphocyte cells can exist with the possibility of irreversible transitions, depending upon the antigen concentration: they have to be associated to a 'virgin', a 'memory' and a 'suppressed' regime state.

REFERENCES

[1] Newsholmes, E.A., Challis, R.A.J. and Crabtree, B. (1984) Trends Biochem. Sci. 9, 277–280.
[2] Katz, J. and Rognstad, R. (1976) Curr. Top. Cell. Regul. 10, 237–289.
[3] Hers, H.G. (1976) Biochem. Soc. Trans. 4, 985–988.
[4] Hue, L. (1982) in: Metabolic Compartmentation (Sies, H. ed.) pp. 71–97, Academic Press, New York.
[5] Bontemps, F., Van den Bergue, G. and Hers, H.G. (1983) Proc. Natl. Acad. Sci. USA 80, 2829–2833.
[6] Challiss, R.A., Arch, J.R.S. and Newsholmes, E.A. (1984) Biochem. J. 221, 153–161.
[7] Hers, H.G. (1976) Annu. Rev. Biochem. 45, 167–189.
[8] Stalmans, W. (1976) Curr. Top. Cell. Regul. 11, 51–97.

[9] Häussinger, D. and Sies, H. (1979) Eur. J. Biochem. 101, 179–184.

[10] Häussinger, D., Gerok, W. and Sies, H. (1983) Biochim. Biophys. Acta 755, 272–278.

[11] Steinberg, D. (1963) in: Control of Lipid Metabolism (Grant, J.K. ed.) pp. 111–138, Academic Press, New York.

[12] Newsholmes, E.A. and Crabtree, B. (1976) Biochem. Soc. Symp. 41, 61–109.

[13] Nicholls, D.G. and Crompton, M. (1980) FEBS Lett. 111, 261–268.

[14] Atkinson, D.E. (1977) Cellular Energy Metabolism and its Regulation, Academic Press, New York.

[15] Reich, J. and Sel'Kov, E.E. (1981) Energy Metabolism of the Cell: a Theoretical Treatise, Academic Press, New York.

[16] Hofmeyr, J.H.S., Kaczer, H. and Van der Merwe, K.J. (1986) Eur. J. Biochem. 155, 631–641.

[17] Newsholmes, E.A. and Start, C. (1973) Regulation of Metabolism, John Wiley, London.

[18] Stadtman, E.R. and Chock, P.B. (1978) Curr. Top. Cell. Regul. 13, 53–95.

[19] Goldbeter, A. and Koshland, D.E., jr (1981) Proc. Natl. Acad. Sci. USA 78, 6840–6844.

[20] La Porte, D.C. and Koshland, D.E., jr (1983) Nature 305, 286–290.

[21] Cimino, A. and Hervagault, J.F. (1987) Biochem. Biophys. Res. Commun. 149, 615–620.

[22] Ricard, J. and Soulié, J.M. (1982) J. Theor. Biol. 95, 105–121.

[23] Hervagault, J.F. and Canu, S. (1987) J. Theor. Biol. 127, 439–449.

[24] Babloyantz, A. and Nicolis, G. (1972) J. Theor. Biol. 34, 185–199.

[25] Hahn, H.S., Ortoleva, P. and Ross, J. (1973) J. Theor. Biol. 41, 503–552.

[26] Monod, J. and Jacob, F. (1961) Cold Spring Harb. Symp. Quant. Biol. 26, 389–481.

[27] Rashevsky, N. (1960) Mathematical Biophysics, Dover, New York.

[28] Novick, A. and Wiener, M. (1957) Proc. Natl. Acad. Sci. USA 43, 553–556.

[29] Cohn, M. and Horibata, K. (1959) J. Bact. 78, 601–612.

[30] Eisen, H., Brachet, P., Pereira da Silva, L. and Jacob, F. (1970) Proc. Natl. Acad. Sci. USA 66, 855–859.

[31] Kaufman, M. and Thomas, R. (1987) J. Theor. Biol. 129, 141–162.